

Topological frequency shift of quantum oscillation in CaFeAsF

Taichi Terashima,^{1,*} Shinya Uji,¹ Teng Wang,^{2,3} and Gang Mu^{2,3,†}

¹*International Center for Materials Nanoarchitectonics,
National Institute for Materials Science, Tsukuba 305-0003, Japan*

²*State Key Laboratory of Functional Materials for Informatics,
Shanghai Institute of Microsystem and Information Technology,
Chinese Academy of Sciences, Shanghai 200050, China*

³*CAS Center for Excellence in Superconducting Electronics (CENSE), Shanghai 200050, China*
(Dated: March 26, 2025)

Shubnikov-de Haas oscillation measurements were performed on CaFeAsF up to a high temperature of $T = 7$ K. The oscillation frequency of the α Dirac electron cylinder exhibits a T^2 shift as the temperature is raised, while that of the β Schrödinger hole cylinder shows no clear shift. The observed shift is reasonably explained by the topological frequency shift proposed in [Guo, Alexandradinata, *et al.*, arXiv:1910.07608] which argues that the energy dependence of the effective mass peculiar to a linear band dispersion gives rise to a frequency shift proportional to T^2 . The present result corroborate the applicability of the topological frequency shift to distinguish topologically nontrivial pockets from trivial ones.

Quantum oscillation arising from Landau quantization of electron motion in magnetic fields is a powerful tool to investigate electronic structures of metals. It dates back to 1930 when quantum oscillation in the electrical resistance and magnetization in Bi was observed [1, 2]. Since the Onsager relation [3] and Lifshitz-Kosevich formula [4] to interpret the quantum oscillation were established in 1950s, it has been used to determine the Fermi surface of not only elemental metals [5] but also heavy fermions [6, 7], high-Tc cuprates [8], and so on. The latest field of its application is topological materials. Topological surface states of topological insulators were successfully observed in quantum-oscillation measurements [9, 10]. Further, Dirac or Weyl fermions in topological semimetals can in principle be identified by detecting the Berry phase in quantum-oscillation measurements [11, 12]. However, the necessary procedure is involved even if it is not impossible to perform.

To be specific, we focus on Shubnikov-de Haas (SdH) oscillation, which is described as follows [5, 13]:

$$\frac{\Delta\rho}{\rho_0} = -C\sqrt{B}R_T R_D R_s \cos\left[2\pi\left(\frac{F}{B} - \frac{1}{2}\right) + \phi_D + \phi_B\right], \quad (1)$$

where $\Delta\rho$ is the oscillatory part of resistivity, while ρ_0 is the background resistivity. We have neglected harmonics. C is a positive coefficient. The frequency F is related to a Fermi-surface cross sectional area A as $F = (\hbar/2\pi e)A$. The temperature and Dingle reduction factors are given by $R_T = X/\sinh X$ and $R_D = \exp(-X_D)$, where $X_{(D)} = K\mu^*T_{(D)}/B$, $\mu^* = m^*/m_e$, and the coefficient K is 14.69 T/K. The spin reduction factor R_s describes the interference of oscillations from up- and down-spin electrons and is given by $R_s = \cos(\pi g\mu^*/2)$, where g is the conduction-electron g factor averaged over the cyclotron orbit under consideration. ϕ_D is 0 for a two-dimensional (2D) Fermi-surface (FS) cylinder while it is $+$ or $-\pi/4$ when the oscillation is from a minimum or maximum cross section

of a three-dimensional (3D) FS pocket. ϕ_B is the Berry phase, which is 0 for normal (i.e., Schrödinger) fermions but π for Dirac fermions [11, 12].

We note that the phase of quantum oscillation is the same between normal fermions with a negative R_s and Dirac fermions with a positive R_s . Therefore, if we like to determine the Berry phase from experimental data by making a Landau-index plot or fitting Eq. 1 to the data, we first have to determine the sign of R_s . R_s depends on g and m^* . g may substantially deviate from the free-electron value $g = 2$, especially for small orbits: e.g. for the Zn needle, $g > 100$ is generally accepted [5]. g could be determined by e.g. the spin-zero method in some special cases [14], but it is impossible in most cases. Note that even in noncentrosymmetric crystals, in which double degeneracy of electronic bands is lifted, R_s (or its equivalent) has to be considered as long as time-reversal symmetry is preserved because oscillations from a time-reversal pair of orbits interfere [15]. Clearly, a different approach is required.

Recently, Guo, Alexandradinata, *et al.* (hereafter GAM *et al.* after the three corresponding authors) proposed a new approach [16]. They pointed out that quantum-oscillation frequency from Dirac/Weyl pockets should exhibit a characteristic temperature dependence. The cyclotron effective mass m^* is defined as $m^* = (\hbar^2/(2\pi))|\partial A/\partial E|$. Accordingly, $\partial m^*/\partial E$ is zero for a quadratic band dispersion but finite for a linear dispersion: assuming $E = \hbar vk$, where v is the Fermi velocity, $m^* = |E|/v^2$ and $|\partial m^*/\partial E| = 1/v^2$, that is, as $|E|$ decreases both A and m^* decrease. At a finite temperature T , the Fermi edge broadens, and hence the system might be viewed as a sum of hypothetical systems with the Fermi energy distributed over a range of $\sim k_B T$ around E_F . Since oscillation from smaller orbits with smaller m^* survives to higher temperatures, the effective frequency might decrease. They extended the

Lifshitz-Kosevich formula to the next order in $k_B T/E_F$ and showed that the above expectation is indeed the case (see also [17]):

$$F(T) = F_0 - \frac{(\pi k_B T)^2}{4\beta} \frac{1}{m^*} \left| \frac{\partial m^*}{\partial E} \right|, \quad (2)$$

where F_0 is the frequency at $T = 0$ and $\beta = e\hbar/(2m^*)$. They analyzed quantum oscillation from Dirac pockets in Cd_3As_2 and LaRhIn_5 and demonstrated that Eq. 2 combined with another small correction to $F(T)$, which will be described later, could explain the experimentally observed temperature dependence of the frequencies.

In this article, we apply the GAM method to SdH oscillation in CaFeAsF , an iron-base superconductor parent compound. The Fermi surface in CaFeAsF is composed of a pair of α Dirac electron cylinders and a β Schrödinger hole cylinder [14]. By virtue of the quasi-two-dimensional electronic structure, the sign of R_s was unambiguously determined for both α and β orbits in our previous SdH study and the Berry phase $\pi(0)$ was confirmed for α (β) orbits. In the present study, we performed new SdH measurements up to higher temperatures and extracted the temperature dependence of the α and β frequencies. We will show that the observed temperature dependence can be explained with Eq. 2.

CaFeAsF single crystals A and B were prepared in Shanghai by a CaAs self-flux method [18]. The resistivity was measured along the c axis, and the magnetic field up to 17.5 T was applied along the c axis. The sample temperature was varied between 0.03 and 7 K in a dilution refrigerator. At each temperature, the magnetic field was ramped up to 17.5 T and then down to zero, and thus two magnetoresistivity curves (B -up and B -down) were obtained. No hysteresis was observed and B -up and B -down curves agreed well at all temperatures.

Figure 1(a) shows the (B -up) magnetoresistivity in crystal A measured at $T = 0.03$ K together with its second field derivative. SdH oscillations are clearly visible. The Fourier transform of the second derivative in $1/B$ shows two peaks, corresponding to the α and β frequencies [Fig. 1(b)]. The inset shows the temperature dependence of the oscillation amplitudes. Fits to the temperature reduction factor R_T (solid lines) give the effective masses $m_\alpha^* = 0.404(5) m_e$ and $m_\beta^* = 0.87(2) m_e$, which are consistent with our previous results [14].

In order to precisely determine the frequencies, we fit experimental data ρ_{exp} assuming that each oscillatory component follows Eq. 1 (Fig. 2). The fit function is $\rho_{\text{fit}} = \rho_0(1 + \Delta\rho_\alpha/\rho_0 + \Delta\rho_\beta/\rho_0)$, where ρ_0 is given by a third-order polynomial. As determined in our previous study [14], R_s is positive and $\phi_D = 0$ for both frequencies, while $\phi_B = \pi$ and 0 for α and β , respectively. We fix the effective masses at the above values. The remaining parameters are F , T_D , and a proportionality factor C' ($=CR_s$) for each component. We first fit the average of the B -up and B -down data at $T = 0.03$ K with

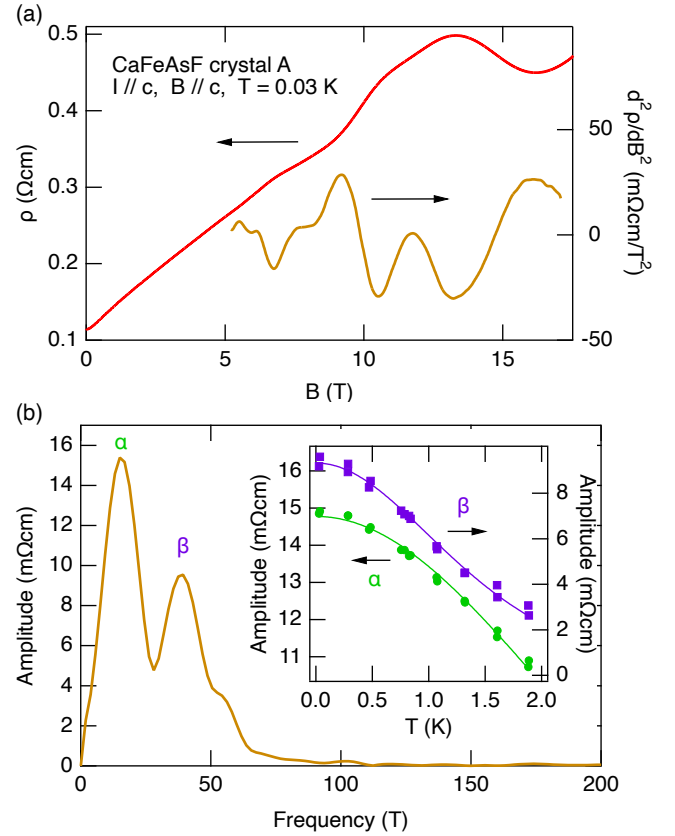


FIG. 1. (a) Magnetoresistivity in crystal A and its second field derivative. (b) Fourier transform of $d^2\rho/dB^2$ vs $1/B$. (inset) Temperature dependence of α and β oscillation amplitudes. The solid lines are fits to R_T .

those fitting parameters (Fig. 2). We obtain $(F, T_D) = (16.510(2) \text{ T}, 5.51(1) \text{ K})$ and $(40.470(3) \text{ T}, 2.05(2) \text{ K})$ for α and β , respectively. From m^* and F , we can estimate the Fermi energies: $E_\alpha = 9.5 \text{ meV}$ and $E_\beta = 5.4 \text{ meV}$, which are measured from the Dirac point and the top of the hole band, respectively. We then fit B -up and B -down data at temperatures up to $T = 3.1$ K, separately, with the values of T_D and C' fixed at those obtained at $T = 0.03$ K: accordingly there is only one fitting parameter F for each component. The β component is very small at $T = 3.1$ K (Fig. 2). At $T = 4.0$ K and above, whether β is included or not does not affect the quality of fit and hence we omit β . The obtained temperature shift of the frequencies are shown in Fig. 4, where the lowest-temperature ($T = 0.03$ K) frequencies are used as F_0 . Note that there are two data points at each temperature corresponding to B -up and B -down sweeps. While ΔF_α is negative and proportional to T^2 , ΔF_β is nearly zero. The B -up and B -down values of F_β at $T = 3.1$ K, which corresponds to $T^2\mu^2/F_0 = 0.18 \text{ K}^2\text{T}^2$, differ considerably, which is ascribed to the small oscillation amplitude as noted above.

We now turn to crystal B. Figure 3(a) shows the (B -

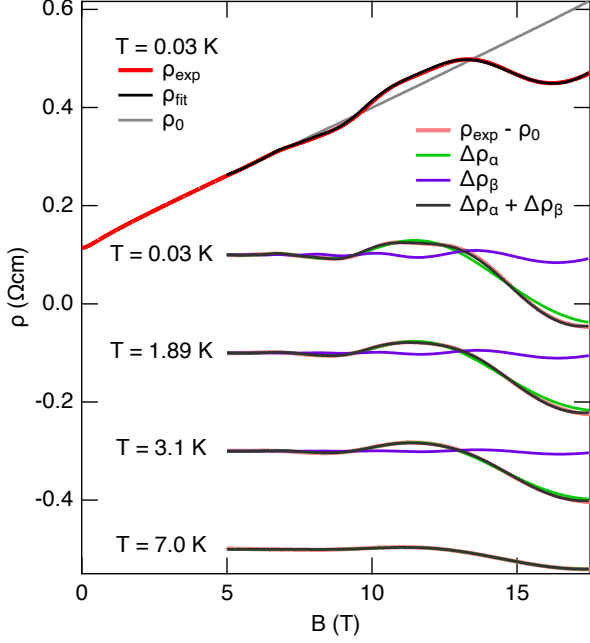


FIG. 2. Lifshitz-Kosevich fits to the magnetoresistivity in crystal A for selected temperatures. For $T = 0.03$ K, the total resistivity ρ_{exp} and oscillatory part $\rho_{exp} - \rho_0$, where ρ_0 is the smooth background, are shown. For the other temperatures, only the oscillatory parts are shown.

up) magnetoresistivity in crystal B at $T = 0.03$ K together with its second field derivative. Although a local maximum of $d^2\rho/dB^2$ near $B = 13$ T is a trace of the β oscillation, the Fourier transform indicates that the α oscillation almost entirely dominates the signal [Fig. 3(b)]. From the temperature dependence of the oscillation amplitude, $m_\alpha^* = 0.397(5) m_e$ is deduced.

We found that a fitting procedure like one used above for crystal A did not work for crystal B: The $\rho(B)$ curve of crystal A exhibits a kink and a local minimum near $B = 9$ and 16 T, respectively [Fig. 1(a)], which define one period of the α oscillation and allow unambiguous determination of F_α by fitting. The $\rho(B)$ curve of crystal B exhibits a kink near $B = 10$ T but no corresponding minimum: the minimum occurs above the highest measured field [Fig. 3(a)]. This introduces ambiguity in determination of F_α by fitting especially at elevated temperatures where the low-field kink also becomes blurred.

We therefore use the phase-shift method to determine the temperature dependence of F_α . In this method, we observe a position of the n -th oscillation minimum or maximum from the infinite field (n is arbitrary) [19, 20]. If the peak occurs at a field $B(T)$ at a temperature T , we can compute the corresponding frequency shift as $(F(T) - F_0)/F_0 = (B(T) - B_0)/B_0$ (see Eq. 1), where F_0 and B_0 are the frequency and peak field at zero temperature, respectively. For this method to work, a signal

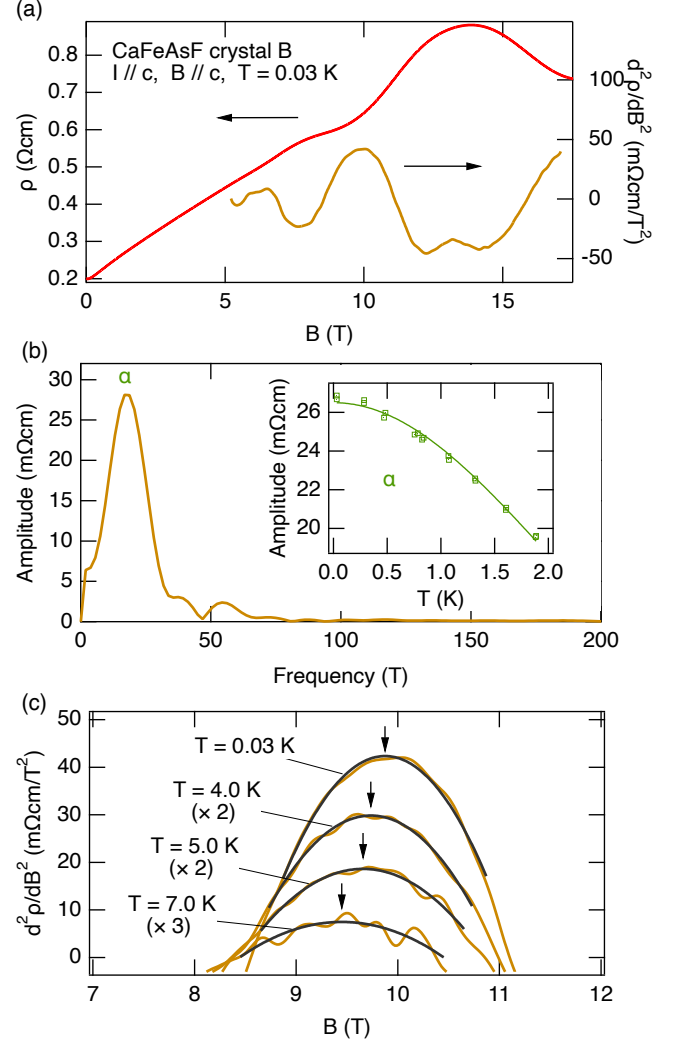


FIG. 3. (a) Magnetoresistivity in crystal B and its second field derivative. (b) Fourier transform of $d^2\rho/dB^2$ vs $1/B$. (inset) Temperature dependence of α oscillation amplitudes. The solid line is a fit to R_T . (c) Second derivative curves at selected temperatures. A second-order polynomial was fit to precisely determine the peak position (arrows).

to be analyzed has to be dominated by a single frequency, which condition is satisfied in the present case.

Figure 3(c) shows the second derivative curves (B -up) at selected temperatures. We fit a second-order polynomial to each curve near its peak to determine the peak field (arrow), which shifts toward lower fields as the temperature increases. We estimate the corresponding frequency shift using the above formula (F_0 was determined from a Lifshitz-Kosevich to the $T = 0.03$ K data). The result is plotted in Fig. 4. The temperature shifts of the α frequency estimated for the two crystals are in good agreement.

We now discuss our main results shown in Fig. 4. GAM *et al.* indicated that the temperature window to observe

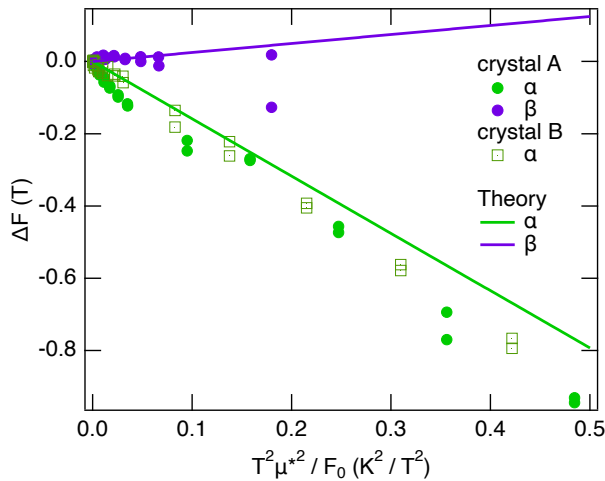


FIG. 4. Experimental (marks) and theoretical (lines) frequency shifts in CaFeAsF.

the topological frequency shift is $0.1 < T\mu^* < 10$ [16]. The present temperature range is compatible with it. GAM *et al.* also noted that, in order to make a quantitative assessment of experimental frequency shifts, it is necessary to consider a frequency shift due to the temperature dependence of the chemical potential (dubbed Sommerfeld correction). Following GAM *et al.* [16], we introduce a parameter Θ and rewrite Eq. 2 as follows:

$$F(T) = F_0 - \Theta \left(\frac{\pi k_B}{\mu_B} \right)^2 \frac{T^2 (\mu^*)^2}{F_0}, \quad (3)$$

where μ_B is the Bohr magneton. The topological shift is given by $\Theta^T = 1/16$. On the other hand, the temperature dependence of the chemical potential is given by

$$\zeta(T) = E_F - \frac{1}{6} (\pi k_B T)^2 \frac{D'}{D}, \quad (4)$$

where D and D' are the zero-field density of states and its energy derivative, respectively. The corresponding frequency shift can be calculated by $\Delta F = (+/-)(m^*/(e\hbar))\Delta\zeta$ (electron/hole). When evaluating Eq. 4. all existing Fermi pockets have to be included. GAM *et al.* considered two extreme cases [16]: One is Cd₃As₂, which has only small Dirac pockets. D is solely determined by those pockets, which gives $\Theta^S = 1/24$. The other is a tiny Dirac pocket in LaRhIn₅, which coexists with much larger Schrödinger ones. In this case, D'/D is dominated by the latter pockets with an effective Fermi energy much larger than measurement temperatures, and hence $\Delta\zeta$ is negligibly small, i.e., $\Theta^S = 0$. The experimental frequency shifts in the two compounds were excellent agreement with those expected from the sum of Θ^T and Θ^S .

The present case is more general. We have to consider the α Dirac and β Schrödinger cylinders at the same time:

$D = 2D_\alpha + D_\beta$ since there are two α cylinders in the Brillouin zone. We make a two-dimensional approximation. Then, the density of states is proportional to the effective mass. Further, $D'_\alpha/D_\alpha = 1/E_\alpha$, and $D'_\beta = 0$. Accordingly, $D'/D = (2/(2 + (m_\beta^*/m_\alpha^*))(1/E_\alpha))$, which leads to $\Theta_\alpha^S = (1/(2 + r))(1/24)$ and $\Theta_\beta^S = -(R/(2 + r))(1/12)$ with $r = m_\beta^*/m_\alpha^*$ and $R = E_\beta/E_\alpha$. Using the effective masses and Fermi energies estimated above, the corresponding lines are plotted in Fig. 4. They explain the experimental shifts reasonably well and confirm topologically nontrivial and trivial nature of the α and β cylinders, respectively. Although the agreement between experiment and theory is not so perfect as in GAM *et al.*, it is not surprising considering crude approximations employed above. We especially note that the present Fermi energies E_α and E_β are more than one order-of-magnitude smaller than that in Cd₃As₂ and less than half of that of the Dirac pocket in LaRhIn₅ considered in GAM *et al.* [16]. Accordingly, our SdH measurements were performed closer to the quantum limit, which fact should be treated properly to improve the theoretical predictions.

To conclude, we performed SdH measurements on CaFeAsF from $T = 0.03$ K to a high temperature of $T = 7$ K. The SdH frequency of the α Dirac cylinder showed a T^2 shift as the temperature is raised, while that of β shows no clear shift. The observed shift can be explained by the topological frequency shift proposed by GAM *et al.* [16] and confirm the topologically nontrivial (trivial) nature of the former (latter) cylinder. The present result extends the applicability of the GAM method from originally tested two extremes where only one Dirac pocket exists or a tiny Dirac pocket coexists with much larger pockets that suppress the chemical potential shift to more general cases, i.e., compensated semimetals with similarly sized electron and hole pockets, which are more relevant to real Dirac/Weyl semimetals.

This work was supported in Japan by JSPS KAKENHI Grant Numbers 17K05556. This work was supported in China by the Youth Innovation Promotion Association of the Chinese Academy of Sciences (No. 2015187).

* TERASHIMA.Taichi@nims.go.jp

† mugang@mail.sim.ac.cn

- [1] V. L. Schubnikow and W. J. de Haas, Proc. Netherlands Roy. Acad. Sci. **33**, 130 (1930).
- [2] W. J. de Haas and P. M. van Alphen, Proc. Netherlands Roy. Acad. Sci. **33**, 1106 (1930).
- [3] L. Onsager, Phil. Mag. **43**, 1006 (1952).
- [4] I. M. Lifshitz and A. Kosevich, Sov. Phys. JETP **2**, 636 (1956).
- [5] D. Shoenberg, *Magnetic Oscillations in Metals* (Cambridge University Press, Cambridge, 1984).
- [6] P. H. P. Reinders, M. Springford, P. T. Coleridge,

- R. Boulet, and D. Ravot, *Phys. Rev. Lett.* **57**, 1631 (1986).
- [7] L. Taillefer and G. G. Lonzarich, *Phys. Rev. Lett.* **60**, 1570 (1988).
- [8] N. Doiron-Leyraud, C. Proust, D. LeBoeuf, J. Levallois, J.-B. Bonnemaïson, R. Liang, D. A. Bonn, W. N. Hardy, and L. Taillefer, *Nature* **447**, 565 (2007).
- [9] D.-X. Qu, Y. S. Hor, J. Xiong, R. J. Cava, and N. P. Ong, *Science* **329**, 821 (2010).
- [10] J. G. Analytis, R. D. McDonald, S. C. Riggs, J.-H. Chu, G. S. Boebinger, and I. R. Fisher, *Nature Physics* **6**, 960 (2010).
- [11] G. P. Mikitik and Y. V. Sharlai, *Phys. Rev. Lett.* **82**, 2147 (1999).
- [12] G. P. Mikitik and Y. V. Sharlai, *Soviet Physics–JETP* **87**, 747 (1998).
- [13] F. E. Richards, *Phys. Rev. B* **8**, 2552 (1973).
- [14] T. Terashima, H. T. Hirose, D. Graf, Y. Ma, G. Mu, T. Hu, K. Suzuki, S. Uji, and H. Ikeda, *Phys. Rev. X* **8**, 011014 (2018).
- [15] H. T. Hirose, T. Terashima, T. Wada, Y. Matsushita, Y. Okamoto, K. Takenaka, and S. Uji, *Phys. Rev. B* **101**, 245104 (2020).
- [16] C. Guo, A. Alexandradinata, C. Putzke, A. Estry, T. Tu, N. Kumar, F.-R. Fan, S. Zhang, Q. Wu, O. V. Yazyev, K. R. Shirer, M. D. Bachmann, H. Peng, E. D. Bauer, F. Ronning, Y. Sun, C. Shekhar, C. Felser, and P. J. W. Moll, arXiv:1910.07608 (2019).
- [17] J.-Y. Fortin and A. Audouard, *The European Physical Journal B* **88**, 225 (2015).
- [18] Y. Ma, H. Zhang, B. Gao, K. Hu, Q. Ji, G. Mu, F. Huang, and X. Xie, *Supercond. Sci. Technol.* **28**, 085008 (2015).
- [19] I. M. Templeton and D. Shoenberg, *Proceedings of the Royal Society of London. Series A. Mathematical and Physical Sciences* **292**, 413 (1966).
- [20] H. Aoki, N. Kimura, and T. Terashima, *Journal of the Physical Society of Japan* **83**, 072001 (2014).